First published January 28, 2016; doi:10.1152/ajprenal.00461.2015.

Modulation of the myogenic mechanism: concordant effects of NO synthesis inhibition and O_2^- dismutation on renal autoregulation in the time and frequency domains

Nicholas G. Moss, Tayler K. Gentle, and William J. Arendshorst

Department of Cell Biology and Physiology, School of Medicine, University of North Carolina at Chapel Hill, Chapel Hill, North Carolina

Submitted 15 October 2015; accepted in final form 21 January 2016

Moss NG, Gentle TK, Arendshorst WJ. Modulation of the myogenic mechanism: concordant effects of NO synthesis inhibition and O_2^- dismutation on renal autoregulation in the time and frequency domains. *Am J Physiol Renal Physiol* 310: F832–F845, 2016. First published January 28, 2016; doi:10.1152/ajprenal.00461.2015.—Renal blood flow autoregulation was investigated in anesthetized C57Bl6 mice using time- and frequency-domain analyses. Autoregulation was reestablished by 15 s in two stages after a 25-mmHg step increase in renal perfusion pressure (RPP). The renal vascular resistance (RVR) response did not include a contribution from the macula densa tubuloglomerular feedback mechanism. Inhibition of nitric oxide (NO) synthase [N^G-nitro-L-arginine methyl ester (L-NAME)] reduced the time for complete autoregulation to 2 s and induced 0.25-Hz oscillations in RVR. Quenching of superoxide (SOD mimetic tempol) during L-NAME normalized the speed and strength of *stage 1* of the RVR increase and abolished oscillations. The slope of *stage 2* was unaffected by L-NAME or tempol. These effects of L-NAME and tempol were evaluated in the frequency domain during random fluctuations in RPP. NO synthase inhibition amplified the resonance peak in admittance gain at 0.25 Hz and markedly increased the gain slope at the upper myogenic frequency range (0.06–0.25 Hz, identified as *stage 1*), with reversal by tempol. The slope of admittance gain in the lower half of the myogenic frequency range (equated with *stage 2*) was not affected by L-NAME or tempol. Our data show that the myogenic mechanism alone can achieve complete renal blood flow autoregulation in the mouse kidney following a step increase in RPP. They suggest also that the principal inhibitory action of NO is quenching of superoxide, which otherwise potentiates dynamic components of the myogenic constriction in vivo. This primarily involves the first stage of a two-stage myogenic response.

renal circulation; perfusion pressure; renal vascular resistance; admittance gain; afferent arteriole

MOST VASCULAR BEDS REGULATE blood flow according to metabolic conditions to provide adequate nutrient delivery and effective waste removal. Control of renal blood flow (RBF) is unique among peripheral vascular beds, as the principal goal is not to satisfy metabolic demands, but rather to stabilize glomerular capillary pressure at a level that provides an adequate glomerular filtration rate. This is achieved by an efficient autoregulatory mechanism(s) that adjusts glomerular afferent arteriolar diameter in response to fluctuations in renal perfusion pressure (RPP). Of equal importance, this process protects glomerular capillaries from excessive pressures that can cause barotrauma, glomerular injury, and renal failure. Several intrinsic mechanisms regulate renal vascular resistance (RVR) in response to changes in RPP (3, 13). In common with most organs, changes in RPP invoke an intrinsic myogenic mechanism in the vascular smooth muscle cells (VSMC) of renal resistance vessels, which stabilizes downstream capillary pressures. The unusually high efficiency of blood flow autoregulation in the kidney may be due to an exceptionally strong myogenic mechanism and perhaps the unique contribution of additional mechanisms involving tubuloglomerular feedback (TGF), such as distal tubular macula densa (MD) cell signaling to the afferent arteriole, termed MD-TGF (3, 13).

Classically, autoregulation has been assessed by determining RBF responses to progressive increases or decreases in RPP with pressure steps lasting 1–2 min to define steady-state autoregulation (13, 15, 33). This produces a static, integrated autoregulatory response that provides an index of overall efficiency, but it does not differentiate between the relative contributions of individual mechanisms. Alternative approaches have analyzed dynamic components of the RPP/RBF relationship in either the time or the frequency domain to isolate the contributions of multiple mechanisms operating in the kidney. The results of these dynamic analyses have revealed distinct components adjusting RVR or vascular admittance based on different time constants of the more rapid myogenic mechanism and the slower MD-TGF mechanism. In the time domain, the increases in RVR to an abrupt step increase in RPP reveals distinct phases or stages in the rate of the response that have been attributed to the sequential operation of the myogenic mechanism followed by input from MD-TGF. In the frequency domain, spectral analysis of relative changes in RBF vs. RPP (admittance gain) distinguish between the operation of the myogenic mechanism at the upper end of the autoregulatory frequency range (0.08–0.25 Hz) and the MD-TGF mechanism at the lower end of the frequency range (0.01–0.02 Hz) (13, 15, 18, 33). In addition, both approaches have advanced evidence suggesting the operation of a third and perhaps even a fourth mechanism (13, 34, 36).

The relative contributions of the myogenic and MD-TGF mechanisms to RBF autoregulation and their interactivity are important questions that remain somewhat controversial. In general, most transfer function studies identify one frequency range for the myogenic response and one for MD-TGF, operating at roughly one cycle every 5 and 30 s, respectively. However, there are examples of RBF autoregulation when two stages are observed in the frequency band encompassing the myogenic response (0.08–0.2 Hz) (41, 89, 91). A third component has been identified in the frequency domain operating at 0.01 Hz (81). In the time domain, the RVR adjustments to a

Address for reprint requests and other correspondence: W. J. Arendshorst, Dept. of Cell Biology and Physiology, School of Medicine, Rm. 6341B, Medical Biomolecular Research Bldg., CB#7545, Chapel Hill, NC 27599-7545 (e-mail: arends@med.unc.edu).

rapid step increase in RPP generally reveal three stages, with transition points at ~5 and 20 s, with achievement of complete RBF autoregulation between 20 and 90 s, suggesting the participation of two or three components (13, 24, 25, 33, 34). The most rapid increase in RVR to a step increase in RPP occurs within the initial 4–5 s and is commonly accepted to represent the myogenic response. A second stage is noted between 5 and 20 s and may represent the myogenic mechanism in the absence of MD-TGF (25) or MD-TGF (19, 20, 34–37). In some studies, RBF is completely autoregulated by 15–25 s with a two-stage increase in RVR (24, 25, 95, 96). In others, a slower third stage is observed between 25 and 60 s (19, 20, 27, 34–37). The mechanism mediating the third component, if evident, is not known. It usually reaches completion by 60 s and may represent MD-TGF, as it can be abolished by inhibition of MD-TGF with a loop diuretic (34–36).

Nitric oxide (NO) appears to exert a pronounced blunting effect on the strength and possibly the rate of the myogenic response. In the time domain, NO synthase (NOS) inhibition by N^G-nitro-L-arginine methyl ester (L-NAME) increases the speed and magnitude of the myogenic response such that complete RBF autoregulation is attained within 10 s (19, 20, 33, 35, 37, 95). In the frequency domain, the myogenic response between 0.08 and 0.25 Hz becomes stronger as indicated by a greater and more rapid decrease in admittance gain in that frequency range (79, 80, 88). In contrast to NO, increased superoxide anion (O_2^-) is a positive modulator of myogenic tone in isolated afferent arterioles (49, 50, 76) and arteriolar constriction stimulated by MD-TGF (54, 75, 93, 94), at least under steady-state conditions. Increased RPP increases O_2^- production by arteries and arterioles (44, 84), including the renal afferent arteriole (50). However, the influence of O_2^- on the dynamic characteristics of RBF autoregulatory mechanisms is not known, in either the presence or absence of NO.

In the present studies, we have integrated time and frequency domain-based approaches to provide a more comprehensive and definitive picture of the autoregulatory response to RPP changes in the mouse kidney. An important feature of our in vivo investigation is the development of functional correlates between the time and frequency domains to assess the roles of NO and O_2^- in paracrine modulation of renal autoregulatory mechanisms by inhibiting NO synthesis with L-NAME and O_2^- dismutation with tempol. We have identified two stages in the myogenic response, independent of MD-TGF, and provide new information about the differential actions of NOS inhibition with L-NAME and O_2^- dismutation with tempol on the initial, most rapid myogenic component. The data suggest that NO attenuates the myogenic response largely by interfering with the vasoconstrictor action of O_2^- and supports a previously unrecognized direct role for O_2^- in regulating the dynamic characteristics of the myogenic autoregulatory response.

METHODS

Male C57Bl6 mice bred in our facility consumed an irradiated commercial rodent diet containing 0.1% NaCl (Teklad 2920X) and drank tap water ad libitum. All experimental protocols and procedures were approved by the institutional animal use and care committee at the University of North Carolina at Chapel Hill and conformed to National Institutes of Health Guidelines for the Care and Use of Laboratory Animals.

Preparation of animals. Animals were anesthetized with an intraperitoneal injection of pentobarbital sodium (60 mg/kg body wt) and placed on a heated operating table with servo-control to maintain body temperature at 37°C. The trachea was intubated with a PE-90 cannula to facilitate spontaneous breathing. A jugular vein was cannulated with three PE-10 catheters for infusion of maintenance solutions, test agents, and supplemental doses of anesthetic. Isotonic saline was infused continuously intravenously at 7 μl/min, and 2% BSA in saline at 3 μl/min (Fraction V, Sigma). RPP was equated with arterial pressure (AP) monitored from a femoral artery with a pressure transducer (Statham p23dB) connected to a Hewlett Packard carrier amplifier (model 8805B). Urine was drained through a PE-90 cannula secured in the bladder at the dome. The right kidney was exposed through a retroperitoneal incision, and the renal artery mobilized free of connective tissue to allow installation of an ultrasonic transit time flow probe (0.5PSB transducer connected to a TS420 flow monitor; Transonic). Renal nerves were removed during this procedure to eliminate reflex sympathetic input to the kidney that could influence RBF during alterations in RPP.

RPP and RBF were digitized at 120 Hz with a sample-and-hold A/D converter (Data Translation, DT9816 A/D board) and displayed on a PC monitor using a data acquisition program based on the DtEZ program suite (Data Translation). At noncritical times, data were averaged in 1-s bins. During data collection periods for analysis of autoregulatory responses, the incoming RPP and RBF data streams were smoothed with a low-pass Butterworth fifth-order digital filter with the frequency cutoff set to 2 Hz and then down-sampled to 10 Hz for storage on disk. Data were collected for 3- or 35-min periods during time-domain and frequency-domain analyses, respectively.

Regulation of RPP by aortic snare. RPP was regulated by adjusting the tension applied to a snare of 8-0 silk suture (0.025 mm diameter) threaded around the abdominal aorta rostral to the right renal artery. After placement around the aorta, the two ends of the snare were tied together, attached to 6-0 suture thread, and drawn through an 18-gauge trocar bent into a rounded 70° angle. A short length of PE-160 tubing was used as an interface between the tip of the trocar and the aorta. The hub of the trocar was clamped to a micromanipulator, and the suture emerging from the hub was attached to a second micromanipulator positioned in line with the trocar. The PE-160 tubing at the trocar tip was positioned adjacent to the aorta so that aortic diameter could be regulated by applying tension to the snare with the second micromanipulator without causing physical disturbance to the surrounding tissue. The 8-0 suture generated minimal friction within the trocar and allowed rapid, unimpeded dilatation of the aorta upon abrupt release of tension. In this way, RPP measured at the femoral artery could be reduced precisely and released rapidly by adjusting the tension on the snare.

Assessment of autoregulation dynamics in the time domain. Dynamic renal autoregulatory efficiency was assessed from the RVR response to an abrupt 20- to 25-mmHg step increase in RPP, as described previously (34–37). Briefly, RPP was reduced from the basal level by tightening the aortic snare until a 20- to 25-mmHg reduction was achieved. RPP was maintained at this level for 1 min before the snare was quickly released to cause RPP to rebound rapidly back to the basal level. The reduced RPP was always maintained within the autoregulatory range (≥80 mmHg); a trial was discontinued if RBF showed a sustained decrease below control levels during the RPP reduction period. Autoregulatory progress was assessed at 0.1-s intervals after the RPP step by calculating the extent to which complete autoregulation was achieved at that time expressed as a percentage of perfect autoregulation. The RVR necessary for perfect autoregulation was obtained by dividing average RPP in the second minute after release by the average RBF before release. In this approach, a perfect autoregulatory response to the RPP step would require no change in RBF and produce 100% autoregulatory effi-

ciency at every time point in the measurement period. Conversely, if RBF increased in direct proportion with the RPP step, there would be no autoregulation, and autoregulatory efficiency would remain at 0% for all measurement times. In the mice studied here, autoregulation reached 100% efficiency within 15 s after the RPP step during control conditions.

Assessment of autoregulation dynamics in the frequency domain. After installation of the aortic snare, the thread passing between the two micromanipulators was linked to the plunger of a 0.25-ml glass tuberculin syringe positioned vertically directly below the snare thread. A length of PE-320 tubing linked the syringe to a water-filled chamber pressurized by a rubber diaphragm connected to a Ling Shaker motor (Ling Dynamic Systems, model 203). Random pressure fluctuations in the syringe were produced by driving the Ling motor with a white noise signal after conditioning with a 2-Hz low-pass filter. The resulting motion of the syringe plunger was delivered to the aorta via tension on the snare to produce random changes in RPP. Digitized and filtered RPP and RBF signals were collected for 35 min and stored on disk for offline analysis.

The RPP and RBF time series data were processed by fast Fourier transformation using repetitive 4,096 sample segments that were normalized to zero mean and detrended. According to Welch's method (92), data segments were overlapped by 50% to reduce noise and variance. Segments were tapered at each end using a Kaiser window with a shape factor set to approximate a normal Gaussian curve. Eight fast Fourier transformations of RBF and RPP data were obtained during each experimental period. The transforms were subjected to cross-spectral analysis to provide measurements of admittance gain, phase relationships, and coherence values for RBF and RPP. An admittance gain of 1.0 is equivalent to 0 dB and corresponds to equivalent power in RBF and RPP oscillations. Gain values below unity signify attenuated power in RBF oscillations relative to RPP, which is indicative of active RBF autoregulation at a given frequency band. Admittance gain values above unity indicate augmented RBF oscillations relative to RPP, perhaps caused by a decrease in RVR due to passive vascular dilation during the pressure wave. The phase relationship between RPP and RBF routinely generated positive phase angles, since RBF oscillations always preceded the corresponding change in RPP. This has been reported in previous studies on the renal and cerebral vasculature (18) and is consistent with the vasculature operating as a high-pass filter with respect to blood flow oscillations (22). Coherence between RBF and RPP spectra represents the fraction of the variance of the RBF signal at a given frequency that can be accounted for on the basis of a linear operation on the RPP signal at that frequency. Coherence would be unity, if there were no variables other than RPP affecting RBF, assuming no measurement error.

Experimental protocols. Experiments were divided into three periods. Control data were obtained in the first period, followed by administration of the NOS inhibitor L-NAME (25 mg/kg iv) in the second period. In the third period, the cell-permeable SOD mimetic tempol was infused (4 $mg \cdot kg^{-1} \cdot min^{-1}$ iv) to produce suppression of superoxide activity during NOS inhibition. A 20-min stabilization period was allowed after L-NAME administration and the start of tempol infusion. In time-domain studies, four RPP steps were performed in each period. Results were averaged in each period to provide three averaged responses for each animal. The same basic protocol was followed in frequency-domain experiments. Data were collected at 10 Hz for 35 min in the control, L-NAME, and combined L-NAME + tempol periods. Derived data from transfer function analyses for each animal were averaged from the eight data segments extracted from each collection period.

Our interpretation of results obtained during L-NAME is based on its inhibitory action on NOS and consequent reduction in NO production and local concentration of NO. L-Arginine analogs, such as L-NAME or N^G-nitro-L-arginine, are known to act as specific inhibitors of NOS isoforms and NO production in health (46, 73). Arginine analogs are commonly used to test the effect of reduced NO on steady-state (8, 29, 58) and dynamic characteristics (32, 35, 91) of RBF autoregulation in healthy kidneys. Renal NOS enzymes are tonically active under basal conditions, and NOS inhibition is associated with reductions in renal tissue NO concentration and urinary excretion of the NO metabolites nitrate/nitrite (43, 57, 59–61). Acute suppression of NO production leads to increased AP, renal vasoconstriction, decreased RBF, and reduced sodium excretion (46, 48, 63, 73, 77). These effects can be reversed by excess L-arginine or a NO donor, such as sodium nitroprusside or cell-permeable 8-bromo-cGMP (42, 48, 59, 62, 74). NOS inhibition also attenuates acetylcholine-induced urinary excretion of cGMP, an index of renal NOS activity, and the concomitant renal vasodilation (8, 82). These effects are independent of the constrictor actions of angiotensin II (ANG II) or the sympathetic nervous system, at lease in conscious, unstressed animals (7, 46, 73).

The contribution of MD-TGF to the autoregulatory response was tested in other mice by blocking MD-TGF with ureteral obstruction (UO) during an osmotic diuresis. To induce the diuresis, a 10% wt/vol solution of mannitol in 0.45% saline was infused intravenously at a rate of 20 μl/min. When urine flow had increased from the basal level of 1–2 to 20–30 μl/min, the right ureter was tied off at the renal pelvis. After 10 min for equilibration, experiments proceeded with step increases or random fluctuations in RPP.

In a separate series of experiments, the RPP step protocol was performed before and during intravenous infusion of arginine vasopressin (AVP) titered to produce an increase in RPP equal to that caused by L-NAME treatment (300 ng/min at 30 μl/min). These data controlled for effects of increased RPP caused by L-NAME that were unrelated to NO inhibition. A second series tested the direct effect of the hypotensive action of tempol on the autoregulatory response after treatment with L-NAME in the frequency domain. In these mice, tempol was omitted from the third period, and instead the aortic snare was tightened to reduce mean RPP to the control level. Random fluctuations were induced at this mean pressure in the manner described.

Data analysis: time domain. The increase in RVR following a RPP step was expressed as the percent return to 100% autoregulation based on the RBF and RPP values before the RPP step. The resulting RVR response curves were analyzed up to 60 s following the RPP step. An initial rapid decrease and increase in RVR over the first 0.7 s were excluded from the analysis, as this has been identified as a passive response to the initial surge in pressure within the vasculature (34, 96). Many studies on rodents have shown that the restoration of RBF following the RPP step occurs in discrete stages that can be attributed to the operation of individual components in the autoregulatory response (27, 34, 96). Two distinct stages were evident in the RVR responses in our animals, with 100% efficiency generally occurring during the second stage ~15 s after the RPP increase. The slopes for each stage and transition points were analyzed by multiple-regression analysis to produce best fit data using commercial software (Prism 6.5, Graphpad software). To provide unambiguous identification of slopes and time points, the transition point between *stages 1* and *2* was constrained to occur no sooner than 1 s after the RPP step. A second transition point was set to occur no earlier than 15 s, which provided a value corresponding to the end of *stage 2*. Slopes and transition points in each period were compared by two-way ANOVA or by *t*-test where appropriate. The overall autoregulatory efficiency was assessed by comparisons of mean RBF during 60 s of reduced RPP immediately before the RPP step and mean RBF between 90 and 120 s after the RPP step. The efficiency of steady-state RBF autoregulation was equated with the efficiency recorded between 50 and 60 s.

Data analysis: frequency domain. The imposed fluctuations in RPP required persistent tension on the aortic snare. Thus mean RPP in these experiments was ~10 mmHg lower than the basal or spontaneous RPP in the absence of aortic occlusion.

Transfer function analyses of RPP and RBF were performed on data derived from the real and imaginary components of their cross

spectrum, which constitute the cospectrum and quadrature spectrum, respectively. Phase angle was calculated from the arctangent of the cospectrum and quadrature spectrum at each frequency step and expressed in degrees. Admittance gain was calculated as the square root of summed squares of the cospectrum and quadrature spectrum and adjusted to correct for the large difference between raw RPP and RBF values. The correction factor was calculated as the ratio of average fluctuation amplitudes in untransformed RPP and RBF traces. Coherence was calculated as the squared cross-spectral density factored by the product of RPP and RBF autospectral densities at each frequency step and expressed on a ratio scale between 0 and 1.

Comparisons of the slopes of admittance gain in the 0.06- to 0.2-Hz frequency range associated with the myogenic mechanism were made using a linear frequency scale. This provided more resolution and the opportunity to perform multiple regression analyses of the slope values using the same procedure as described for the RPP step response. The minimum value for the transition point between two stages was set to occur at no less than 0.155 Hz.

Chemicals used. Pentobarbital, L-NAME, tempol, and AVP were obtained from Sigma Chemical.

RESULTS

Average body weight of all animals in the study was 28.2 ± 0.5 g, with a right kidney weight of 0.216 ± 0.005 g ($n = 40$). During control conditions, mean AP was 105 ± 2 mmHg, and RBF averaged 8.58 ± 1.51 ml·min^{-1}·g kidney wt^{-1}.

The mean autoregulatory efficiency curve of RVR following a 25-mmHg step increase in RPP during the control state is shown in Fig. 1*A*. The trace shows the time course for reestablishment of autoregulation over the first 60 s after the RPP step from 80 to 105 mmHg. The RVR response curve had several distinct phases, beginning with an immediate decline for 0.3 s, followed by a sharp rebound between 0.3 and 0.7 s (Fig. 1*A*, *inset*). These initial RVR changes have been attributed to passive distension and subsequent elastic recoil of the vasculature caused by the immediate impact of the RPP increase (96). The passive nature of this immediate response is confirmed by its persistence after elimination of the active autoregulatory response by calcium channel blockers (34). The active autoregulatory RVR response was composed of two distinct stages with a transition at ~5 s (Fig. 1). Each stage contributed ~50% of the RVR response, leading to perfect autoregulation that was attained by ~13 s. The second stage continued beyond 100% and ended at 19 s after the RPP step, with a total efficiency of 115%. Mean slope values for the two stages, transition points, and completion times for the second stage are given in Table 1. The prestep RPP and RBF values were mean values over 60 s immediately before the RPP step. The poststep RPP and RBF values were recorded between 90 and 120 s after the

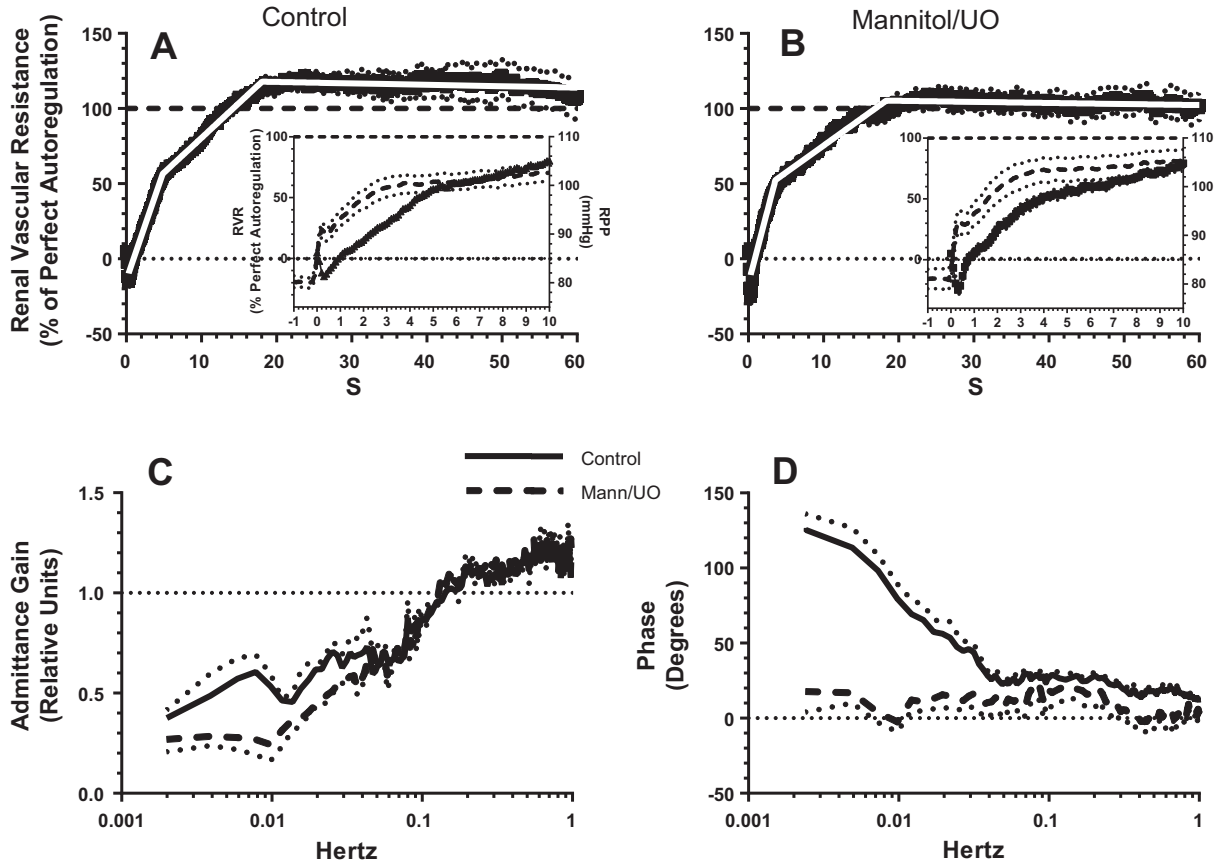

Fig. 1. Changes in renal vascular resistance (RVR) in the time domain in response to a step increase in renal perfusion pressure (RPP) before (*A*) and during inhibition of macula densa-tubuloglomerular feedback (MD-TGF) with mannitol + ureteral obstruction (UO; *B*) ($n = 7$ mice). *Insets* magnify changes in the first 10 s after the RPP increase showing RVR (solid lines) and BP (dashed lines). Changes are shown in admittance gain (*C*) and phase (*D*) in the frequency domain during random oscillations in RPP before (solid line) and during inhibition of MD-TGF with mannitol + UO (dashed line) (8 mice). Values are means ± SE (dotted lines).

Table 1. *Renal vascular resistance response to a RPP step increase before and during inhibition of macula densa-tubuloglomerular feedback inhibition with mannitol and complete unilateral ureteral obstruction*

	RPP, mmHg		RBF, ml·min^{-1}·g KW^{-1}		Slope, %/s		Termination Point, s	
	Prestep	Poststep	Prestep	Poststep	*Stage 1*	*Stage 2*	*Stage 1*	*Stage 2*
Control	80 ± 1	105 ± 2	7.3 ± 0.6	7.2 ± 0.6	15.3 ± 0.9	4.7 ± 0.2	4.7 ± 0.3	18.1 ± 0.3
Mannitol/UO	81 ± 1	105 ± 2	5.8 ± 0.5	6.0 ± 0.5	19.6 ± 1.2*	3.7 ± 0.2	3.5 ± 0.1	18.4 ± 0.4

Values are means ± SE; $n = 7$ mice. RPP, renal perfusion pressure; RBF, renal blood flow; KW, kidney weight; UO, ureteral obstruction. *$P < 0.001$ vs. control.

RPP step. It is clear that that RBF was efficiently autoregulated over this time frame. The fact that RBF ended up slightly lower than the prestep starting level suggests an element of super-autoregulation.

To determine the contribution of MD-TGF to the RVR response in the time domain, similar experiments were performed after inhibition of MD-TGF by means of a 10% mannitol diuresis, combined with complete ureteral occlusion (mannitol/UO) (18). As is shown in Fig. 1*B*, inhibition of MD-TGF did not change the general shape of the RVR response, which achieved 100% efficiency by 13–14 s. Thus the initial two stages of the autoregulatory adjustments in RVR persisted after suppression of MD-TGF and are most likely exclusively due to a myogenic mechanism(s). In the absence of MD-TGF, each stage still accounted for ~50% of perfect autoregulation. Nevertheless, it is noteworthy that there was a 28% increase in the slope of *stage 1* ($P < 0.001$), whereas the slope of *stage 2* decreased insignificantly (Table 1). Unlike the control state, during mannitol/UO the final autoregulatory RVR response did not exceed 100% of perfect autoregulation (Fig. 1*B*). These findings suggest that MD-TGF exerted a small inhibitory effect on the initial myogenic response, probably due to a dilatory action of MD-TGF during the reduced RPP that tended to offset the initial RVR increase when RPP was abruptly increased. Also, the MD-TGF mechanism appeared to be implicated in an RVR overshoot beyond 100% efficiency that was commonly observed between 15 and 60 s in trials when MD-TGF was active, contributing to a small increase in RVR after completion of the myogenic response.

Our interpretation of the myogenic mechanism(s) being the major, if not exclusive, contributor to RBF autoregulation under the described experimental conditions depends on the effectiveness of mannitol/UO in inhibiting MD-TGF. This was tested by transfer function analysis of renal vascular admittance. Admittance gain derived from the transfer function during control conditions and mannitol/UO is shown in Fig. 1*C*. Reading the traces from right to left, control admittance gain showed a steep decline beginning at 0.2 Hz, the corner frequency for onset of the renal myogenic autoregulatory response (15, 18, 33). Admittance gain then plateaued at 0.06 Hz, with a second decline beginning at 0.025 Hz. The latter is commonly identified as the onset of the MD-TGF mechanism (2, 18, 30, 52). A third gain reduction occurred at very low frequencies (0.005 Hz), but the coherence between the RBF and RPP signals in this range was too low to permit confident interpretation.

We observed that mannitol/UO did not affect the slope of the myogenic response between 0.2 and 0.06 Hz, whereas the change in admittance gain associated with MD-TGF activity at lower frequencies was virtually eliminated (Fig. 1*C*). Effective abrogation of MD-TGF by mannitol/UO was also evident in the elimination of a pronounced increase in phase angle present in the control state at frequencies associated with MG-TGF activity (Fig. 1*D*). An increasing phase angle in this frequency range indicates an increasing independence of RBF from the passive effects of RPP fluctuations, consistent with strong MD-TGF activity. These findings extend previous studies showing that full autoregulatory efficiency can be achieved by myogenic mechanisms without the involvement of MD-TGF (18, 30).

To assess the role of NOS inhibition on the dynamic characteristics of the renal myogenic mechanism(s), the RPP step protocol was repeated after L-NAME inhibition of NOS activity and NO production. Dramatic effects were observed in both the time- and frequency-domain experiments. Renal autoregulatory efficiency in the time domain increased to 170% within 2 s after the RPP step (Fig. 2). This rapid increase in RVR constituted the first upswing of a pronounced oscillatory re-

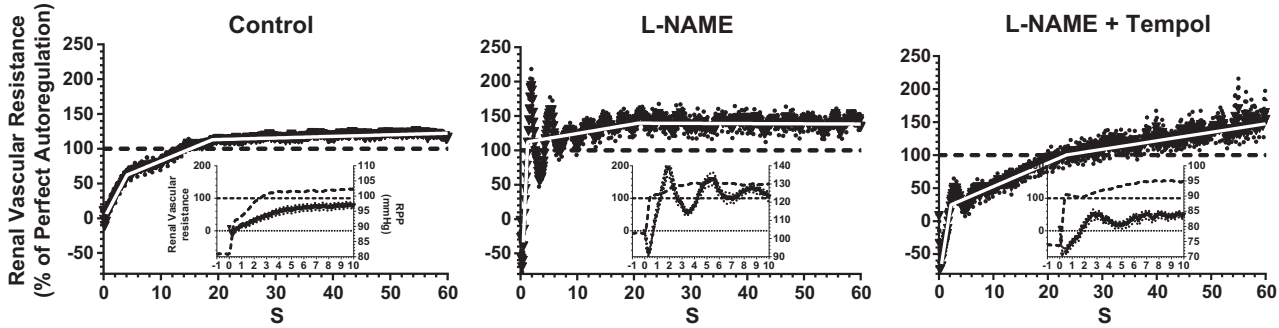

Fig. 2. Changes in RVR in the time domain in response to a step increase in RPP before (*left*) and during the inhibition of nitric oxide synthase (NOS) activity by N^G-nitro-L-arginine methyl ester (L-NAME; *middle*) and during NOS inhibition plus quenching of superoxide anion (O_2^-) by tempol (*right*). *Insets* show the first 10 s of the RVR response, including the initial passive stages and the onset of the active myogenic response (solid lines, *left* axes) and RPP (dashed lines, *right* axes). Values are means ± SE (dotted lines; $n = 9$ mice).

Table 2. *Effects of L-NAME and tempol on the autoregulatory responses of renal vascular resistance to a RPP step*

	RPP, mmHg		RBF, ml·min^{-1}·g KW^{-1}		Slope, %/s		Termination Point, s	
	Prestep	Poststep	Prestep	Poststep	*Stage 1*	*Stage 2*	*Stage 1*	*Stage 2*
Control	82 ± 1	106 ± 1	9.4 ± 0.6	9.0 ± 0.6	15.5 ± 0.8	3.4 ± 0.1	4.12 ± 0.16	19.0 ± 0.3
L-NAME	103 ± 1	129 ± 1	2.8 ± 0.4	2.6 ± 0.4	188.3 ± 21.3†	1.4 ± 0.2	1.23 ± 0.06	0.8 ± 1.7
L-NAME + tempol	74 ± 1	97 ± 1	2.2 ± 0.4	2.0 ± 0.4	52.6 ± 6.7†	3.6 ± 0.2	2.20 ± 0.03	3.5 ± 1.1*

Values are means ± SE; n = 9 mice. L-NAME, N^G-nitro-L-arginine methyl ester. *$P < 0.01$ and †$P < 0.001$ vs. control.

sponse at a frequency of 0.25 Hz, which persisted for 1–2 min with progressively diminishing amplitude. Following the initial *stage 1* rise in RVR during L-NAME, the mean slope during oscillations was not different from the slope of *stage 2* in the control response and terminated at the same point after the RPP step. This indicates that the oscillatory response originated in *stage 1* and persisted throughout *stage 2* as a modulating effect on the slope of the underlying response.

Additional experiments tested the notion that the effects of NOS inhibition were due, at least in part, to the enhanced vasomotor activity of O_2^-. To this end, we infused the cell-permeable SOD mimetic tempol during L-NAME inhibition of NOS. Slopes and transition points of the RVR responses to the step change in RPP during control, L-NAME, and L-NAME + tempol periods are shown in Fig. 2 and are summarized in Table 2. In essence, superoxide inhibition with tempol reversed the stimulatory action noted during NOS inhibition on the initial rate of the myogenic autoregulatory response (*stage 1*) and virtually eliminated the oscillations in RVR following the RPP step, consistent with a major potentiating action of O_2^- on *stage 1* of myogenic vasoconstriction in the absence of NO. *Stage 2* of the myogenic response was similar to that observed during control conditions. The data indicate that that NO synthesis inhibition leads to an exaggerated myogenic response. The exaggerated myogenic response was normalized by tempol, an effect suggesting an exaggerated vasoconstrictor action of O_2^- during NOS inhibition.

The increase in basal AP from 105 to 128 mmHg after L-NAME is a consideration, as this alone might influence the rate of the autoregulatory response (90). This was tested by repeating the RPP step in a separate group of mice before and during intravenous infusion of AVP at a rate that produced a stable increase in AP similar to that produced by L-NAME. The general pattern of the autoregulatory response in these AVP-infused mice at 126 mmHg was not different from the control response seen at the basal pressure of 100 mmHg, and no oscillations in RVR occurred following the RPP step. These results are presented in Fig. 3 and Table 3. There was an increase in the slope of *stage 1* from 17.7 to 28.6%/s ($P < 0.001$). This may reflect a relatively small enhancement of the myogenic response due to the increased RPP compared with the effects of NOS inhibition with L-NAME on the *stage 1* slope (increase from 15.5 to 188.3%/s) when RPP increased to a similar extent. The duration of *stage 1* was reduced after AVP, leading to a transition to *stage 2* at 2.8 s vs. 4.2 s during control conditions. This also might reflect a response to the higher basal RPP. It is notable that there were reciprocal percent changes in the slope and end point of *stage 1* after AVP, suggesting that a similar degree of vasoconstriction was achieved over a shorter time period, which accounted for ~60% of full autoregulatory efficiency. The slope of *stage 2* was not altered during AVP-induced hypertension. These data extend previous results, showing that the dynamics of RBF autoregulation are largely unaffected by hypertension produced by ANG II or phenylephrine (20, 35, 71, 80).

The effects of NOS inhibition followed by superoxide dismutation on the autoregulatory response were investigated further by performing transfer function analyses of RPP/RBF relations. The black trace in Fig. 4*A* shows the complete admittance gain relationship between 0.001 and 1 Hz in the control state. The presence of a myogenic component between 0.2 and 0.06 Hz and MD-TGF between 0.02 and 0.009 Hz was clearly evident. After L-NAME (red trace), a prominent resonance peak appeared in the admittance gain between 0.3 and 0.2 Hz, with a peak 200% above unity at 0.25 Hz. This frequency corresponds to the 0.25-Hz oscillations in RVR caused by NOS inhibition in the time domain. The slope of admittance gain in the myogenic region was clearly increased by L-NAME and resulted in a reduction in relative gain from 2.0 at 0.2 Hz to 0.4 at 0.06 Hz, a gain value that in the control state required the combined operation of MD-TGF and myogenic mechanisms. As in the time domain, the increased magnitude of the myogenic response was largely reversed by tempol (blue trace), which also reduced the amplitude of the resonance peak at 0.25 Hz close to control levels. Inspection of the admittance gain trace between 0.02 and 0.001 Hz after tempol reveals the reappearance of a characteristic MD-TGF signature that was suppressed during L-NAME alone. This suggests that the absence of MD-TGF activity following L-NAME treatment was likely due to enhanced myogenic contractility rather than inhibition of the MD-TGF signaling mech-

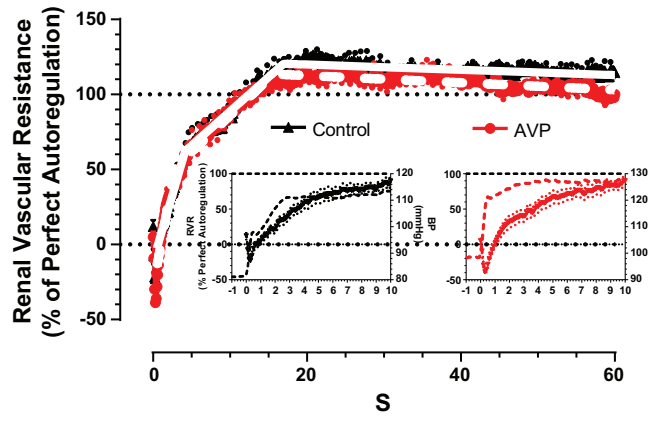

Fig. 3. Changes in RVR in the time domain in response to a step increase in RPP before (control; black) and during acute arginine vasopressin (AVP)-induced vasoconstriction and hypertension (red). *Insets* show the initial 10 s of the RVR response (*left* axes) and RPP (*right* axes). Values are means ± SE (dotted lines; n = 6 mice).

Table 3. *Effect of AVP-induced hypertension on the autoregulatory response of renal vascular resistance to a RPP step*

	RPP, mmHg		RBF, ml·min^{-1}·g KW^{-1}		Slope, %/s		Termination Point, s	
	Prestep	Poststep	Prestep	Poststep	*Stage 1*	*Stage 2*	*Stage 1*	*Stage 2*
Control	77 ± 3	101 ± 4	6.1 ± 0.3	5.9 ± 0.3	17.7 ± 0.8	4.6 ± 0.1	4.2 ± 0.2	17.0 ± 0.2
AVP	98 ± 2	127 ± 3	7.1 ± 1.3	7.3 ± 1.3	28.6 ± 1.6†	4.9 ± 0.1	2.8 ± 0.1*	15.7 ± 0.2

Values are means ± SE; $n = 6$ mice. AVP, arginine vasopressin. *$P < 0.05$ and †$P < 0.001$ vs. control.

anism per se. The mean RPP and RBF values for these experiments are presented in Table 4.

Phase and coherence relationships between RPP and RBF are shown in Fig. 4, *C* and *D*. The phase transition between 0.2 and 0.06 Hz during control conditions was strongly accentuated after NOS inhibition, indicating the increased strength of the myogenic mechanism in this frequency range. This was also the case in the MD-TGF range (<0.025 Hz) after L-NAME, albeit less pronounced, which is consistent with the loss of the MD-TGF signature in admittance gain after L-NAME. Interestingly, the phase relationship between RPP and RBF after tempol was restored to the control level, an observation consistent with the apparent restoration of MD-TGF seen in the admittance gain traces. In the control and L-NAME + tempol periods, coherence was greater or equal to 0.5 for frequencies >0.009 Hz, thus providing strong confidence for the derived parameters at this frequency and above. Coherence was less well sustained at low frequencies during L-NAME alone, coincident with the low admittance gain. This indicates a more complex, nonlinear relationship between RPP and RBF, perhaps fueled by the enhanced action of superoxide on the vascular contractile response.

It is reasonable to expect that the distinct stages apparent in the myogenic response during control, L-NAME, and L-NAME + tempol periods in the time domain are also evident in the frequency domain. To assess this prediction, the section of admittance gain associated with the myogenic response in the frequency domain (0.06–0.25 Hz) was

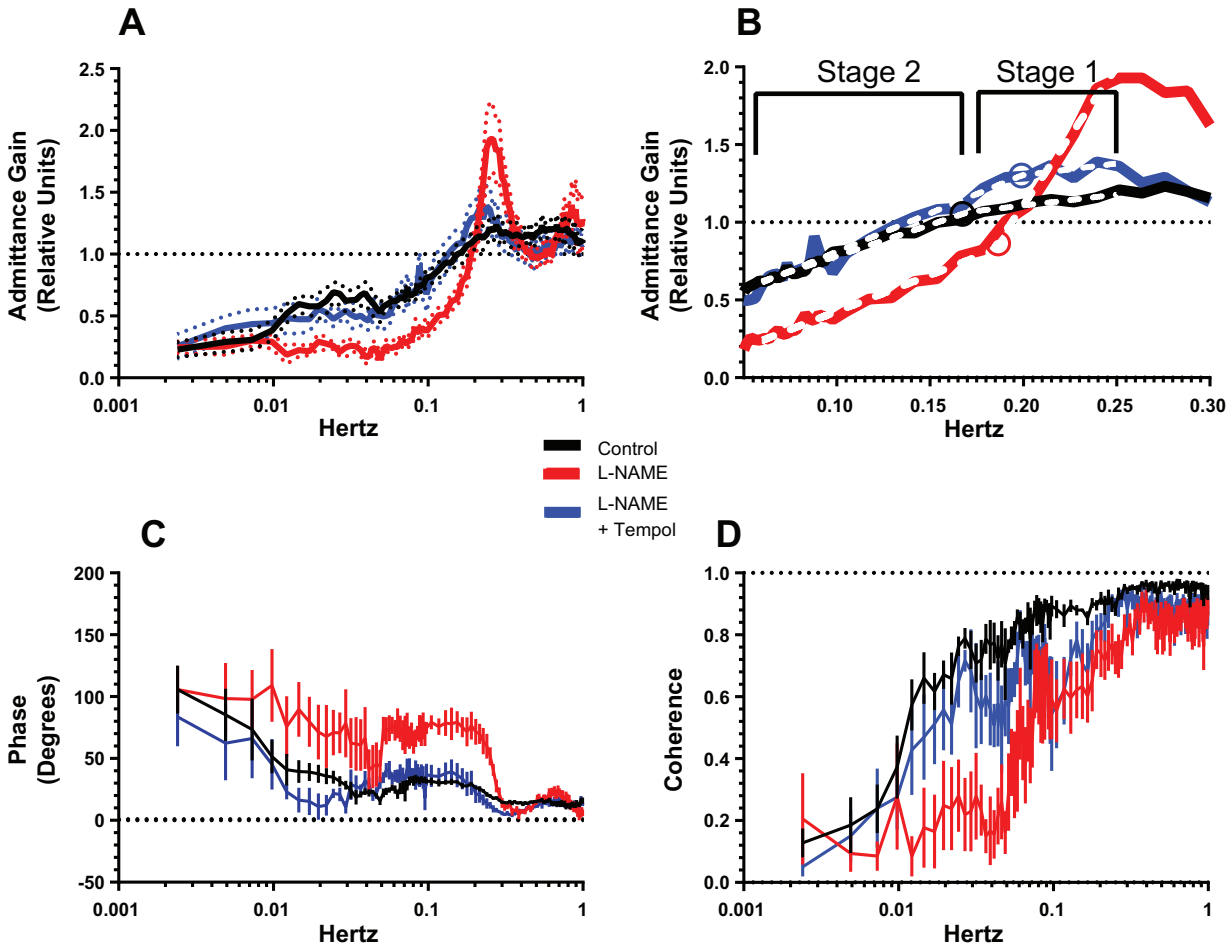

Fig. 4. Changes in admittance gain (*A* and *B*), phase (*C*), and coherence (*D*) in the frequency domain before (control; black), during L-NAME inhibition of NOS (L-NAME; red) alone, and in combination with tempol quenching of O_2^- (L-NAME + tempol; blue). *B*: magnification of changes in admittance gain against a linear scale of frequency between 0.06 and 0.3 Hz, highlighting different slopes of *stages 1* and *2* and the transition point (circles). Values are means ± SE (dotted lines; $n = 6$ mice).

Table 4. *Slopes for the two stages and the transition point between the stages of the renal myogenic response based on a linear frequency scale (Fig. 4B)*

	RPP, mmHg	RBF, ml·min^{-1}·g KW^{-1}	Slope, Δgain/Hz		Transition, Hz
			Stage 1	*Stage 2*	
Control	83 ± 2	5.6 ± 0.6	1.8 ± 0.9	4.2 ± 0.5	0.16 ± 0.02
L-NAME	116 ± 6	2.5 ± 0.3	17.7 ± 2.4*	4.6 ± 0.6	0.18 ± 0.01
L-NAME + tempol	85 ± 2	2.4 ± 0.2	0.8 ± 3.1	4.9 ± 0.5	0.21 ± 0.03

Values are means ± SE; $n = 6$ mice. *$P < 0.001$ vs. control.

magnified in Fig. 4*B* and plotted on a linear frequency axis to facilitate comparisons of the slopes. In view of the two stages characterizing the myogenic mechanism in the time domain, each admittance gain trace was analyzed using multiple linear regression to evaluate differences in slopes and transition points. The transition points for each period were constrained to occur after 0.15 Hz. The resulting best-fit regression lines are shown as dotted lines in Fig. 4*B*, and the slopes and transition points are summarized in Table 4. Two stages were identified in the myogenic frequency range. It is striking that the transition point between stages (identified by circles) was not statistically different among the three experimental periods and that the slopes of myogenic responses in the low-frequency range (labeled as *stage 2*) were the same during the three conditions. The admittance gain for the higher frequency range between 0.15 and 0.25 Hz, labeled *stage 1*, showed a significantly increased slope above control in the L-NAME group, an effect normalized by tempol treatment. We postulate that these two stages in the myogenic response in the frequency domain correspond to the two stages identified in the time domain. In each case, the slope of *stage 1* only was augmented by inhibition of NO and inhibited by suppression of O_2^-. In the time domain, this was the initial stage after the increase in RPP, while in the frequency domain the responsive region was restricted to the higher frequencies of the myogenic range (*stage 1* in Fig. 4*B*). By this reasoning, *stage 2* in Fig. 4*B* was comparable to *stage 2* of the myogenic response in the time domain, both of which were insensitive to L-NAME and tempol.

Tempol treatment after L-NAME during spectral analysis experiments reduced RPP to the control level seen before L-NAME. This is a potential confounding factor in the interpretation of these data, as the RPP drop alone could alter the admittance gain (71, 90). To test this, the admittance gain was determined in other animals before and during NOS inhibition with L-NAME, followed by a period in which fluctuations in RPP were reduced to the mean level recorded during tempol treatment. The admittance gain, phase angle, and coherence of the RPP/RBF relationship for these experiments are presented in Fig. 5. The forced reduction in mean RPP from 118 to 79 mmHg during NOS inhibition with L-NAME caused a small nonsignificant reduction in the magnitude of the admittance gain from 1.6 ± 0.2 to 1.3 ± 0.2 relative units, with a small reduction of the corner frequency at which this occurred by 0.022 Hz. The lower RPP also caused a consistent offset in the myogenic gain response, amounting to −0.034 ± 0.004 Hz between 0.2 and 0.1 Hz. Nevertheless, the overall gain and phase relationships between RPP and RBF after L-NAME were similar at high and normal RPP levels (Table 5).

DISCUSSION

Our study provides a comprehensive description of the dynamic characteristics of blood flow autoregulation in the mouse kidney using a novel combination of time- and frequen-

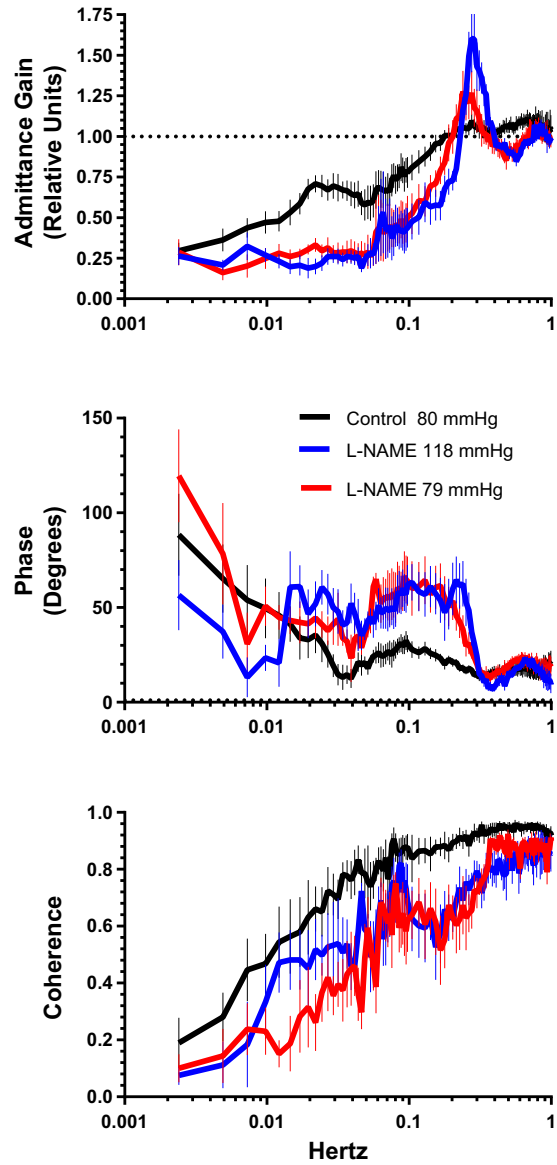

Fig. 5. Changes in admittance gain during control (black), and L-NAME inhibition of NOS when mean RPP was 118 mmHg (red) and then reduced to 79 mmHg by aortic constriction (blue). Values are means ± SE ($n = 6$ mice).

Table 5. *Lack of effect of changing RPP on frequency analysis of admittance gain and resonance frequency during nitric oxide synthase inhibition by L-NAME*

	RPP, mmHg	RBF, ml·min^{-1}·g KW^{-1}	Admittance Gain at Resonance Peak, relative units	Resonance Frequency, Hz
Control	80 ± 2	7.3 ± 0.7	1.1 ± 0.04	0.283 ± 0.002
L-NAME high	118 ± 5	3.2 ± 0.7	1.6 ± 0.2	0.278 ± 0.006
L-NAME low	79 ± 2	2.6 ± 0.4	1.3 ± 0.2	0.256 ± 0.007*

Values are means ± SE; $n = 6$ mice. *$P < 0.001$ vs. control.

cy-domain analyses. We provide new evidence that autoregulatory adjustments in RVR following a step increase in RPP are essentially complete within 15 s and are mediated exclusively by the myogenic mechanism(s). This intrinsic, rapid myogenic response involves two phases or stages that do not require MD-TGF to achieve a complete autoregulatory response. *Stage 1* produces a 50–60% increase in RVR by 3 s, and *stage 2* accounts for the remaining 40–50% by 13 s. A slight overshoot was complete by 18 s. In addition, on the basis of responses to L-NAME and tempol, our data implicate interactive roles for superoxide and NO in the modulation of dynamic elements in myogenic RBF autoregulation in the healthy kidney. As might be expected, inhibition of NO synthesis accentuates the autoregulatory response, presumably by reducing NO-mediated vasodilation. However, subsequent dismutation of the vasoconstrictor O_2^- restores the original speed and strength of the myogenic constrictor response, despite continued NOS inhibition. In this regard, our data support the hypothesis that the predominant action of NO is to suppress a O_2^--mediated vasoconstrictor effect, perhaps secondary to quenching O_2^-, rather than exerting a direct vasodilatory action. A new finding is that these interactions are primarily targeted to the initial, most rapid phase of the myogenic mechanism and have little influence on the second slower phase of myogenic vasoconstriction, or on overall, steady-state RBF autoregulation.

An abrupt increase in RPP has been used previously to investigate dynamic aspects of RBF autoregulation in dogs, rats, and mice. A study on anesthetized dogs showed that RBF returned to the control level 25 s after a 40-mmHg step increase in RPP (31). Similar to our mouse results, Young and Marsh (96) showed that RBF autoregulation in the rat was complete 15 s after a 10- to 20-mmHg RPP step. In their study, an immediate passive response in RVR lasted <1 s, followed by an initial active stage that produced a 50% increase in RVR at ~3 s and a subsequent slower increase in RVR that completed the autoregulatory response by 15 s (96). Measurements of tubular fluid flow changes in the early distal tubule after the RPP step led them to conclude that the rather sluggish MD-TGF response could not operate within the time frame of these autoregulatory RVR responses. Daniels and Arendshorst (17) reached a similar conclusion based on the time delay required for activation and completion of the MD-TGF mechanism. Using stop-flow micropuncture methodology, these investigators found a 15-s delay in the single nephron MD-TGF response following a step change in late proximal tubule perfusion. The MD-TGF response attained 50% of its eventual maximum 27 s after the increase in perfusion rate, which is too slow to participate in the autoregulatory response. This is in accordance with an earlier study showing no measurable effect of MD-TGF inhibition by UO on the static RBF autoregulatory curve (18). In the exposed juxtamedullary preparation of rats, autoregulatory adjustments of afferent arteriolar diameter responded quickly to a step increase in RPP (86). The decrease in diameter took place between 6 and 24 s when MD-TGF was active and between 6 and 13 s during abrogation of MD-TGF by papillectomy. Thus MD-TGF complimented the myogenic response only after 13 s. In the hydronephrotic rat kidney, which lacks tubules and thus any MD-TGF, afferent arteriolar diameter responses to a step increase in RPP were complete within 15 s (56).

Drummond and colleagues (24, 25, 27) performed in vivo RBF studies in anesthetized mice assessing the dynamic changes in RVR to a step increase in RPP. Two rates of change in RVR were noted with complete autoregulation attained in 15–20 s. As we observed, the first active stage took place in the 1- to 5-s time window, and the second stage was completed by 15–20 s after the RPP increase. This was the case whether MD-TGF was normal or inhibited by acute volume expansion (25), indicating a predominant contribution from the myogenic mechanism. Genetic deletion of acid-sensing ion channel 2 proteins or knockdown of epithelial Na channel β-subunit, which are postulated mechanosensors in the renal vasculature, slowed the initial stage by 50% without affecting the second stage (24, 27). It is noteworthy that, in our study, NO and O_2^- inhibition also primarily affected the initial rapid stage (*stage 1*) of the myogenic response. Thus *stage 1* of the myogenic mechanism appears to be selectively responsive to physiological signals compared with the slower second stage that is relatively insensitive. This is similar to earlier observations in other vascular beds that identified two stages in the myogenic response. In that case, an initial, rate-sensitive mechanism preceded a second static response that was not influenced by the rate of pressure change (4, 5, 21).

Our data are consistent with earlier reports showing effective renal autoregulatory response to an abrupt increase in RPP that is complete in 15–25 s after the RPP step in multiple species. Moreover, the data indicate that this is due to a rapid myogenic mechanism without significant contribution from the slower MD-TGF mechanism. In contrast, rodent studies by Just and colleagues (19, 20, 34–36) have shown that the autoregulatory response of RVR was not completed until 50–60 s after a 20-mmHg RPP increase. They identified three active components in the RVR response: an initial active stage lasted 4–5 s, a second stage ending ~20–25 s later, and a third stage taking place between 25 and 60 s. During inhibition of MD-TGF with furosemide, the third stage was abolished in wild-type mice and normal rats, whereas the first two stages persisted in roughly the same time intervals as during control conditions (34–36). Thus, according to our interpretation, their data are consistent with the most rapid two phases being associated with the myogenic mechanism, while the third mechanism is due to MD-TGF. However, their assumption that the myogenic

mechanism takes place between 1 and 4–7 s and that the MD-TGF begins at 4–7 s and ends at 25–30 s (20, 36, 37) is at variance with our conclusion. The persistence of an autoregulatory response in the 5- to 20-s time window during furosemide inhibition of MD-TGF was interpreted as an undefined mechanism, independent of the myogenic and MD-TGF mechanisms, whereas our data clearly establish that RBF autoregulation in this time window is achieved by the second stage of the myogenic response. Ge et al. (25) also find a similar second stage of the RVR response when MD-TGF is inhibited by extracellular fluid volume expansion. It is likely that a marked difference in the time interval required for the completion of RBF autoregulation is the basis of the divergent conclusions, but the underlying reason for the difference is not known.

As previously described (34), our time-domain analysis shows a modulatory action of MD-TGF on the rate of the myogenic mechanism such that the latter was increased when MD-TGF was inhibited. This is likely a function of the experimental design in which reduced RPP before the step increase in RPP reduces flow to the MD and elicits a vasodilatory signal from the MD-TGF mechanism (34). This persists during the first seconds following the step increase in RPP and tends to oppose the initial stage of the rapid increase in RVR mediated by the myogenic mechanism. This was not apparent in the frequency domain, where admittance gain associated with the myogenic mechanism was not altered after MD-TGF inhibition with mannitol/UO. In contrast to the step change in RPP, continuous random fluctuations in RPP do not produce a clear temporal sequence that results in unambiguous interaction between myogenic and MD-TGF components. Thus, when studied in the frequency domain, MD-TGF might not influence admittance gain in the myogenic frequency range of 0.06–0.2 Hz, as has been previously noted by others (2, 18).

Our control values for frequency analysis are consistent with previous studies of renal autoregulation using frequency domain analysis on anesthetized rats. These studies consistently show admittance gain responses with shoulders at 0.2 Hz and 0.02 Hz, which are the transition points attributed to the onset of the myogenic and MD-TGF mechanisms, respectively (13, 15, 18, 33). A previous study by Iliescu et al. (30) in conscious mice found that relative admittance gain fluctuated between 1.8 and 2.5 relative units (5–8 dB) at frequencies >0.2 Hz, whereas our relative admittance gain fluctuated between 1.2 and 1.3 units in the same frequency range. Between 0.2 and 0.1 Hz, the relative admittance gain in conscious mice fell to 0.7 units (−3 dB); our relative admittance gain decreased from 1.2 to 0.7 units over the same frequency range. Thus our data for admittance gain are in close agreement with this earlier study. Also, our data are almost identical to a decrease in relative admittance gain from 1.2 to 0.7 between 0.2 and 0.1 Hz reported for rats anesthetized with pentobarbital (18). In rats anesthetized with isoflurane, Cupples et al. (16) showed relative gain increasing from 1.1 to 1.8 between 0.35 and 0.2 Hz, at which point gain decreased to 0.45 between 0.2 and 0.1 Hz. In a another study using the same protocol, these investigators reported an increase in relative gain from 1.3 to 1.8 between 1.0 and 0.2 Hz and then a decrease to 0.75 (−5 dB) at 0.07 Hz (80). Thus our current data on admittance gain in the control period are in close agreement with previous studies, with the caveat that differences might be expected with respect to species used, state of anesthesia, the kidney preparation, and type of AP fluctuations employed.

The efficiency of steady-state RBF autoregulation, based on the plateau phase, is not affected by NOS inhibition (6, 8, 20, 35, 58, 67), whereas the dynamic components of the myogenic mechanism are clearly influenced by the presence and absence of NO. Changes in the time domain include an accelerated and pronounced increase in RVR with obvious oscillations (Fig. 2) (19, 20, 35, 95). In the frequency-domain, L-NAME caused an exaggerated resonance peak at 0.25 Hz and a stronger myogenic response identified by an accelerated reduction in admittance gain in the myogenic frequency range (Fig. 4) (79, 80, 87, 90, 91). Thus NO inhibition did not affect overall steady-state RBF autoregulation, but did markedly augment the rate at which it is achieved. The potentiation of an intrarenal mechanism(s) appears to be independent of hypertension per se, as the myogenic response is not altered markedly by ANG II, AVP, or phenylephrine-induced hypertension of a magnitude similar to that of NOS inhibition (Fig. 3) (20, 35, 71, 80). Multilinear analysis of the RVR response to the RPP step revealed that the target of NOS inhibition was the initial stage of the myogenic response, which became accelerated and stronger and was converted to oscillations. Such oscillations became superimposed onto the second stage with diminishing amplitude, while the fundamental mean slope of the second stage remains unchanged. This was also evident in the frequency domain when NOS inhibition strongly increased the slope of admittance gain at the higher end of the myogenic range and amplified the resonance peak at 0.25 Hz. At lower frequencies in the myogenic range, between 0.06 and 0.1 Hz, the slope of admittance gain was unaffected by NOS inhibition. A similar two-stage response of admittance gain after L-NAME was seen in rats by Wang and coworkers (88, 89, 91), where distinct regions in admittance gain were noted between 0.25-0.1 Hz and 0.1-0.06 Hz. However, this was not readily apparent during control conditions (88, 89, 91). As noted above, two distinct components or stages in the RVR response in the time domain were also reported by Drummond and colleagues (24, 25, 27) between 3 and 25 s after a RPP step.

In addition to eliciting vasodilation, NO blunts vasoconstriction produced by G protein-coupled agonists, such as ANG II, endothelin-1, and the catecholamines norepinephrine or phenylephrine (9, 38, 40). Exaggerated vasoconstriction by one of these agonists might explain the enhanced myogenic response during NOS inhibition. However, ANG II and catecholamines do not potentiate the myogenic response in the time domain (20, 35) or the frequency domain (1, 71, 80) as markedly as that seen during NOS inhibition of NO production. On the other hand, O_2^- does enhance the myogenic response by an action independent of NO (50). Thus we conclude that NOS inhibition leads to an exaggerated myogenic response that is likely mediated by reduced vasodilatory activity from NO and/or enhanced O_2^--mediated vasoconstriction.

The incorporation of superoxide removal with tempol after NOS inhibition is an important component of our studies, as it probes the direct cause of the increased vascular reactivity associated with L-NAME treatment. The actions of L-NAME may be readily explained by elimination of the vasodilatory actions of NO, but our observations suggest a more complex explanation. The action of L-NAME on the myogenic autoregulatory response was reversed by tempol in both the time and

frequency domains. The opposite actions of NO synthesis inhibition with L-NAME and O_2^- dismutation by tempol suggest counteracting influences of NO and O_2^- on the myogenic mechanism. Such a paracrine-like interaction was apparent during the initial, but not the secondary, stage of the myogenic response in our time-series experiments. In addition, a similar interaction was suggested only at higher frequencies in the myogenic range in spectral analyses of RBF autoregulation, which we have identified in Fig. 4*B* as *stage 1*. Collectively, these findings are consistent with the proposal that the inhibitory action of NO on the myogenic response results from quenching of O_2^- in *stage 1* of the myogenic response and does not involve a direct vasodilatory action involving activation of soluble guanylyl cyclase (sGC) and cGMP production. If this were not the case, one would expect the vasoconstrictor action of L-NAME to persist after O_2^- dismutation with tempol, which was not observed. This is also supported by data showing that tempol alone has a relatively minor effect on the autoregulatory response to a step increase in RPP compared with the pronounced effect after NO inhibition (N. G. Moss and W. J. Arendshorst, unpublished observations). This proposed role for NO is at variance with a recent publication showing that an effect of L-NAME on the myogenic response similar to that reported here was reversed by cGMP formation induced by continual pharmacological stimulation of sGC (19). Overall steady-state RBF autoregulation efficiency was attenuated by up to 33%, although most investigators report that NO donors, L-arginine, or acetylcholine do not affect the efficiency of overall steady-state autoregulation (28, 45, 67, 68). Adding to controversy in this area are the puzzling results on mice deficient in the various NOS isoforms from which Dautzenberg et al. (20) concluded that eNOS activity attenuates the myogenic response in a manner independent of NO production. Physiological NO stimulation by endothelin-induced activation of endothelin B receptors attenuates the myogenic response without affecting overall autoregulation (79). Early studies showed modulation of RPP-induced steady-state constriction of the preglomerular vasculature by cGMP-dependent vasodilators, such as sodium nitroprusside and ANP (11). Other studies suggest cGMP-independent actions, since ANP or administration of L-arginine failed to completely reverse the actions of NOS inhibition on RBF autoregulation and admittance gain in the myogenic frequency range (91). The mechanisms by which NO produces vasodilation of afferent arterioles is concentration dependent, with low concentrations ($<$900 nM) acting through cGMP, whereas higher concentration exerts an effect independent of cGMP (83). There is evidence suggesting that the NO/sGC pathway can cause renal vasodilation via a phosphodiesterase 3 and cAMP-dependent pathway (78). Thus physiological activation of autoregulatory responses by abrupt changes or fluctuations in RPP and shear stress may recruit different pathways from those engaged by constant pharmacological activation of NO.

Several studies on isolated vessels have supported a prominent role for O_2^- in potentiating vasoconstriction in resistance arterioles. Increased luminal pressure rapidly increased NADPH oxidase production of ROS in isolated mouse tail arterioles (66), hamster gracilis muscle arteries (44), carotid arteries (84), cerebral arteries (26), and mouse afferent arterioles (50, 53). This was associated with enhanced myogenic vasoconstriction, perhaps by promoting Ca^{2+} entry or sensitivity of the VSMC contractile apparatus (26, 66). O_2^- facilitates opening of L-type Ca^{2+} channels during VMSC membrane depolarization (85). Studies on isolated mouse afferent arterioles have shown that O_2^- plays an important role in potentiating contractile responses to vasoconstrictors, such as ANG II and thromboxane A_2 (49, 53) and in the steady-state myogenic response to increased intraluminal pressure (49, 50, 53). O_2^- is thought to enhance in vitro renal myogenic contraction largely independent of NO (50), although its actions in modulating MD-TGF appear to be either by limiting bioavailability of NO (54, 93) or a direct action on the afferent arteriole (54). The mutual quenching action between NO and O_2^- limits bioavailability of both radicals and is thought to modulate afferent arteriolar reactivity to ANG II (12). Thus, when both are generated in physiologically relevant amounts, an excess of NO will produce the same response as a deficiency in O_2^-. This might explain steady-state studies reporting no effect of tempol on RPP-induced constriction of the afferent arteriole of the isolated, perfused hydronephrotic kidney (69) or on steady-state autoregulation of RBF and medullary blood flow under basal conditions (23).

We recognize that the use of tempol to inactivate the vasoconstrictor O_2^- by dismutation could result in the generation of the vasodilator H_2O_2, which may play a role in the vasodilatory response. However, we believe that the renal hemodynamic actions of tempol are primarily due to dismutation of O_2^- and the removal of its vasoconstrictor influence rather than increased H_2O_2 levels. This conclusion is based on the published work of other investigators showing that the potentiating action of O_2^- on myogenic vasoconstriction in arteries and arterioles during increased intraluminal pressure is inhibited by tempol, but not by catalase (26, 50). Also, the enhanced myogenic response of afferent arterioles of SHR is normalized by the O_2^- scavenger tempol or by the Nox2 inhibitor gp91ds, findings that led to the conclusion that Nox2-derived O_2^- may contribute to the enhanced myogenic response (76). In mice, isolated afferent arterioles increased O_2^- production in response to increased luminal pressure, which magnified myogenic constriction and was inhibited by tempol but unaffected by catalase, even though exogenous H_2O_2 is reported to blunt the myogenic constriction of renal arterioles (50). Similar observations have been made on the cerebral circulation. Increased luminal pressure in rat middle cerebral arteries increased O_2^- and H_2O_2 generation that resulted in augmentation of myogenic constriction (26). The potentiation was inhibited by tempol in the presence or absence of polyethylene glycol catalase (26), indicating a primary action of O_2^- rather than H_2O_2. Moreover, H_2O_2 commonly acts as vasodilator in circulatory beds, such as cerebral, coronary, mesenteric, and skeletal muscle, and may function as an endothelium-dependent hyperpolarization factor and an activator of potassium channels (10, 14, 47, 55, 64, 70); both dilator and hyperpolarizing actions are expected to blunt rather than potentiate pressure-induced myogenic constriction.

Animal studies have demonstrated that O_2^- dismutation by tempol attenuates renal vasoconstriction induced by ANG II, AVP, endothelin, and norepinephrine, and that this vasoconstrictor action of O_2^- may involve quenching of NO and also an action independent of NO (39, 40, 65). On the other hand, our laboratory (65) has shown previously that O_2^- enhances the renal vasoconstrictor action of AVP primarily by limiting the

bioavailability of NO, suggesting different roles as a function of stimulus. The action of L-NAME on the myogenic autoregulatory response in our studies of renal autoregulation was reversed by tempol in both the time and frequency domain, suggesting a direct vasoconstrictor action of O_2^- in the absence of NO. In isolated mouse afferent arterioles, O_2^- enhances the myogenic constriction by an action independent of NO (50). In addition, a recent modeling study of the actions of NO and O_2^- on the myogenic mechanism in afferent arterioles concludes that activation of sGC by NO is of less importance than the intracellular quenching of O_2^- by NO (51). We believe our observations are consistent with the conclusion that NOS inhibition leads to an exaggerated myogenic response as a result of attenuated NO production, less quenching of O_2^-, and the augmented actions of the vasoconstrictor O_2^-.

Perspectives

Our studies clearly demonstrate that complete autoregulation of RBF following an abrupt RPP step is accomplished in two stages by the autonomous myogenic response of VSMC in the renal microcirculation of mice. While this does not exclude MD-TGF from a role in the autoregulatory response during more gradual pressure changes, abrupt alterations in RPP are effectively countered by the myogenic mechanism within 15 s. Following NOS inhibition, the enhanced speed and strength in *stage 1* appear to be dependent on increased O_2^- bioavailability, as both are reversed by quenching of O_2^- with tempol. These observations provide a new perspective on the control of the myogenic mechanism in RBF autoregulation that has important implications for renal function in conditions of oxidative stress as well as health.

GRANTS

This work was supported by National Heart, Lung, and Blood Institute Research Grant HL-02334.

DISCLOSURES

No conflicts of interest, financial or otherwise, are declared by the author(s).

AUTHOR CONTRIBUTIONS

Author contributions: N.G.M. and W.J.A. conception and design of research; N.G.M., T.E.K., and W.J.A. performed experiments; N.G.M., T.E.K., and W.J.A. analyzed data; N.G.M., T.E.K., and W.J.A. interpreted results of experiments; N.G.M., T.E.K., and W.J.A. prepared figures; N.G.M. and W.J.A. drafted manuscript; N.G.M. and W.J.A. edited and revised manuscript; N.G.M. and W.J.A. approved final version of manuscript.

REFERENCES

1. **Abu-Amarah I, Ajikobi DO, Bachelard H, Cupples WA, Salevsky FC.** Responses of mesenteric and renal blood flow dynamics to acute denervation in anesthetized rats. *Am J Physiol Regul Integr Comp Physiol* 275: R1543–R1552, 1998.
2. **Ajikobi DO, Novak P, Salevsky FC, Cupples WA.** Pharmacological modulation of spontaneous renal blood flow dynamics. *Can J Physiol Pharmacol* 74: 964–972, 1996.
3. **Arendshorst WJ, Navar LG.** Renal Circulation and Glomerular Hemodynamics. In: *Diseases of the Kidney & Urinary Tract*, edited by Schrier RW, Nielsen EH, Molitoris BA, Coffman TM, and Falk RJ. Philadelphia, PA: Lippincott Williams & Wilkins, 2012.
4. **Basar E, Weiss C.** [Analysis of the frequency characteristics of pressure-induced changes in flow resistance of the isolated rat kidney]. *Pflügers Arch* 304: 121–135, 1968.
5. **Basar E, Weiss C.** Rate sensitivity of the mechanism of pressure induced change of vascular resistance. *Kybernetik* 5: 241–247, 1967.
6. **Baumann JE, Persson PB, Ehmke H, Nafz B, Kirchheim HR.** Role of endothelium-derived relaxing factor in renal autoregulation in conscious dogs. *Am J Physiol Renal Fluid Electrolyte Physiol* 263: F208–F213, 1992.
7. **Baylis C, Harvey J, Santmyire BR, Engels K.** Pressor and renal vasoconstrictor responses to acute systemic nitric oxide synthesis inhibition are independent of the sympathetic nervous system and angiotensin II. *J Pharmacol Exp Ther* 288: 693–698, 1999.
8. **Beierwaltes WH, Sigmon DH, Carretero OA.** Endothelium modulates renal blood flow but not autoregulation. *Am J Physiol Renal Fluid Electrolyte Physiol* 262: F943–F949, 1992.
9. **Berthold H, Just A, Kirchheim HR, Ehmke H.** Interaction between nitric oxide and endogenous vasoconstrictors in control of renal blood flow. *Hypertension* 34: 1254–1258, 1999.
10. **Beyer AM, Durand MJ, Hockenberry J, Gamblin TC, Phillips SA, Gutterman DD.** An acute rise in intraluminal pressure shifts the mediator of flow-mediated dilation from nitric oxide to hydrogen peroxide in human arterioles. *Am J Physiol Heart Circ Physiol* 307: H1587–H1593, 2014.
11. **Bouriquet N, Casellas D.** Interaction between cGMP-dependent dilators and autoregulation in rat preglomerular vasculature. *Am J Physiol Renal Fluid Electrolyte Physiol* 268: F338–F346, 1995.
12. **Carlstrom M, Lai EY, Ma Z, Steege A, Patzak A, Eriksson UJ, Lundberg JO, Wilcox CS, Persson AEG.** Superoxide dismutase 1 limits renal microvascular remodeling and attenuates arteriole and blood pressure responses to angiotensin II via modulation of nitric oxide bioavailability. *Hypertension* 56: 907–913, 2010.
13. **Carlstrom M, Wilcox CS, Arendshorst WJ.** Renal autoregulation in health and disease. *Physiol Rev* 95: 405–511, 2015.
14. **Chin LC, Achike FI, Mustafa MR.** Hydrogen peroxide modulates angiotensin II-induced contraction of mesenteric arteries from streptozotocin-induced diabetic rats. *Vascul Pharmacol* 46: 223–228, 2007.
15. **Cupples WA, Braam B.** Assessment of renal autoregulation. *Am J Physiol Renal Physiol* 292: F1105–F1123, 2007.
16. **Cupples WA, Novak P, Novak V, Salevsky FC.** Spontaneous blood pressure fluctuations and renal blood flow dynamics. *Am J Physiol Renal Fluid Electrolyte Physiol* 270: F82–F89, 1996.
17. **Daniels FH, Arendshorst WJ.** Tubuloglomerular feedback kinetics in spontaneously hypertensive and Wistar-Kyoto rats. *Am J Physiol Renal Fluid Electrolyte Physiol* 259: F529–F534, 1990.
18. **Daniels FH, Arendshorst WJ, Roberds RG.** Tubuloglomerular feedback and autoregulation in spontaneously hypertensive rats. *Am J Physiol Renal Fluid Electrolyte Physiol* 258: F1479–F1489, 1990.
19. **Dautzenberg M, Kahnert A, Stasch JP, Just A.** Role of soluble guanylate cyclase in renal hemodynamics and autoregulation in the rat. *Am J Physiol Renal Physiol* 307: F1003–F1012, 2014.
20. **Dautzenberg M, Keilhoff G, Just A.** Modulation of the myogenic response in renal blood flow autoregulation by NO depends on endothelial nitric oxide synthase (eNOS), but not neuronal or inducible NOS. *J Physiol* 589: 4731–4744, 2011.
21. **Davis MJ, Sikes PJ.** Myogenic responses of isolated arterioles: test for a rate-sensitive mechanism. *Am J Physiol Heart Circ Physiol* 259: H809–H900, 1990.
22. **Diehl RR, Linden D, Lucke D, Berlit P.** Phase relationship between cerebral blood flow velocity and blood pressure. A clinical test of autoregulation. *Stroke* 26: 1801–1804, 1995.
23. **Feng MG, Dukacz SA, Kline RL.** Selective effect of tempol on renal medullary hemodynamics in spontaneously hypertensive rats. *Am J Physiol Regul Integr Comp Physiol* 281: R1420–R1425, 2001.
24. **Gannon KP, McKey SE, Stec DE, Drummond HA.** Altered myogenic vasoconstriction and regulation of whole kidney blood flow in the ASIC2 knockout mouse. *Am J Physiol Renal Physiol* 308: F339–F348, 2015.
25. **Ge Y, Gannon KP, Gousset M, Liu R, Murphey B, Drummond HA.** Impaired myogenic constriction of the renal afferent arteriole in a mouse model of reduced β-ENaC expression. *Am J Physiol Renal Physiol* 302: F1486–F1493, 2012.
26. **Gebremedhin D, Terashvili M, Wickramasekera N, Zhang DX, Rau N, Miura H, Harder DR.** Redox signaling via oxidative inactivation of PTEN modulates pressure-dependent myogenic tone in rat middle cerebral arteries. *PLoS One* 8: e68498, 2013.
27. **Grifoni SC, Chiposi R, McKey SE, Ryan MJ, Drummond HA.** Altered whole kidney blood flow autoregulation in a mouse model of reduced beta-ENaC. *Am J Physiol Renal Physiol* 298: F285–F292, 2010.
28. **Gross R, Kirchheim HR, Brandstetter K.** Basal vascular tone in the kidney. Evaluation from the static pressure-flow relationship under normal

autoregulation and at maximal dilation in the dog. *Circ Res* 38: 525–531, 1976.
29. **Hayashi K, Suzuki H, Saruta T.** Nitric oxide modulates but does not impair myogenic vasoconstriction of the afferent arteriole in spontaneously hypertensive rats. Studies in the isolated perfused hydronephrotic kidney. *Hypertension* 25: 1212–1219, 1995.
30. **Iliescu R, Cazan R, McLemore GR Jr, Venegas-Pont M, Ryan MJ.** Renal blood flow and dynamic autoregulation in conscious mice. *Am J Physiol Renal Physiol* 295: F734–F740, 2008.
31. **Jackson TE, Guyton AC, Hall JE.** Transient response of glomerular filtration rate and renal blood flow to step changes in arterial pressure. *Am J Physiol Renal Fluid Electrolyte Physiol* 233: F396–F402, 1977.
32. **Just A.** Nitric oxide and renal autoregulation. *Kidney Blood Press Res* 20: 201–204, 1997.
33. **Just A.** Mechanisms of renal blood flow autoregulation: dynamics and contributions. *Am J Physiol Regul Integr Comp Physiol* 292: R1–R17, 2007.
34. **Just A, Arendshorst WJ.** Dynamics and contribution of mechanisms mediating renal blood flow autoregulation. *Am J Physiol Regul Integr Comp Physiol* 285: R619–R631, 2003.
35. **Just A, Arendshorst WJ.** Nitric oxide blunts myogenic autoregulation in rat renal but not skeletal muscle circulation via tubuloglomerular feedback. *J Physiol* 569: 959–974, 2005.
36. **Just A, Arendshorst WJ.** A novel mechanism of renal blood flow autoregulation and the autoregulatory role of A1 adenosine receptors in mice. *Am J Physiol Renal Physiol* 293: F1489–F1500, 2007.
37. **Just A, Kurtz L, de Wit C, Wagner C, Kurtz A, Arendshorst WJ.** Connexin 40 mediates tubuloglomerular feeback contribution to renal blood flow autoregulation. *J Am Soc Nephrol* 20: 1577–1585, 2009.
38. **Just A, Olson AJ, Falck JR, Arendshorst WJ.** NO and NO-independent mechanisms mediate ETB receptor buffering of ET-1-induced renal vasoconstriction in the rat. *Am J Physiol Regul Integr Comp Physiol* 288: R1168–R1177, 2005.
39. **Just A, Olson AJ, Whitten CL, Arendshorst WJ.** Superoxide mediates acute renal vasoconstriction produced by angiotensin II and catecholamines by a mechanism independent of nitric oxide. *Am J Physiol Heart Circ Physiol* 292: H83–H92, 2007.
40. **Just A, Whitten CL, Arendshorst WJ.** Reactive oxygen species participate in acute renal vasoconstrictor responses induced by ETA- and ETB-receptors. *Am J Physiol Renal Physiol* 294: F719–F728, 2008.
41. **Kada G, Blayney LM, Jeyakumar LH, Kienberger F, Pastushenko VP, Fleischer S, Schindler H, Lai FA, Hinterdorfer P.** Recognition force microscopy/spectroscopy of ion channels: applications to the skeletal muscle Ca2+ release channel (RYR1). *Ultramicroscopy* 86: 129–137, 2001.
42. **Kakoki M, Kim HS, Arendshorst WJ, Mattson DL.** L-Arginine uptake affects nitric oxide production and blood flow in the renal medulla. *Am J Physiol Regul Integr Comp Physiol* 287: R1478–R1485, 2004.
43. **Kakoki M, Zou AP, Mattson DL.** The influence of nitric oxide synthase 1 on blood flow and interstitial nitric oxide in the kidney. *Am J Physiol Regul Integr Comp Physiol* 281: R91–R97, 2001.
44. **Keller M, Lidington D, Vogel L, Peter BF, Sohn HY, Pagano PJ, Pitson S, Spiegel S, Pohl U, Bolz SS.** Sphingosine kinase functionally links elevated transmural pressure and increased reactive oxygen species formation in resistance arteries. *FASEB J* 20: 702–704, 2006.
45. **Kiyomoto H, Matsuo H, Tamaki T, Aki Y, Hong H, Iwao H, Abe Y.** Effect of L-N^G-nitro-arginine, inhibitor of nitric oxide synthesis, on autoregulation of renal blood flow in dogs. *Jpn J Pharmacol* 58: 147–155, 1992.
46. **Kone BC, Baylis C.** Biosynthesis and homeostatic roles of nitric oxide in the normal kidney. *Am J Physiol Renal Physiol* 272: F561–F578, 1997.
47. **Lacza Z, Puskar M, Kis B, Perciaccante JV, Miller AW, Busija DW.** Hydrogen peroxide acts as an EDHF in the piglet pial vasculature in response to bradykinin. *Am J Physiol Heart Circ Physiol* 283: H406–H411, 2002.
48. **Lahera V, Navarro J, Biondi ML, Ruilope LM, Romero JC.** Exogenous cGMP prevents decrease in diuresis and natriuresis induced by inhibition of NO synthesis. *Am J Physiol Renal Fluid Electrolyte Physiol* 264: F344–F347, 1993.
49. **Lai EY, Solis G, Luo Z, Carlstrom M, Sandberg K, Holland S, Wellstein A, Welch WJ, Wilcox CS.** p47(phox) is required for afferent arteriolar contractile responses to angiotensin II and perfusion pressure in mice. *Hypertension* 59: 415–420, 2012.
50. **Lai EY, Wellstein A, Welch WJ, Wilcox CS.** Superoxide modulates myogenic contractions of mouse afferent arterioles. *Hypertension* 58: 650–656, 2011.
51. **Layton AT, Edwards A.** Predicted effects of nitric oxide and superoxide on the vasoactivity of the afferent arteriole. *Am J Physiol Renal Physiol* 309: F708–F719, 2015.
52. **Leyssac PP.** Further studies on oscillating tubulo-glomerular feedback responses in the rat kidney. *Acta Physiol Scand* 126: 271–277, 1986.
53. **Li L, Feng D, Luo Z, Welch WJ, Wilcox CS, Lai EY.** Remodeling of afferent arterioles from mice with oxidative stress does not account for increased contractility but does limit excessive wall stress. *Hypertension* 66: 550–556, 2015.
54. **Liu R, Ren Y, Garvin JL, Carretero OA.** Superoxide enhances tubuloglomerular feedback by constricting the afferent arteriole. *Kidney Int* 66: 268–274, 2004.
55. **Liu Y, Bubolz AH, Mendoza S, Zhang DX, Gutterman DD.** H_2O_2 is the transferrable factor mediating flow-induced dilation in human coronary arterioles. *Circ Res* 108: 566–573, 2011.
56. **Loutzenhiser RD, Bidani AK, Chilton L.** Renal myogenic response: kinetic attributes and physiological role. *Circ Res* 90: 1316–1324, 2002.
57. **Majid DSA, Godfrey M, Grisham MB, Navar LG.** Relation between pressure natriuresis and urinary excretion of nitrate/nitrite in anesthetized dogs. *Hypertension* 25: 860–865, 1995.
58. **Majid DSA, Navar LG.** Suppression of blood flow autoregulation plateau during nitric oxide blockade in canine kidney. *Am J Physiol Renal Fluid Electrolyte Physiol* 262: F40–F46, 1992.
59. **Majid DSA, Omoro SA, Chin SY, Navar LG.** Intrarenal nitric oxide activity and pressure natriuresis in anesthetized dogs. *Hypertension* 32: 266–272, 1998.
60. **Majid DSA, Said KE, Omoro SA.** Responses to acute changes in arterial pressure on renal medullary nitric oxide activity in dogs. *Hypertension* 34: 832–836, 1999.
61. **Majid DSA, Said KE, Omoro SA, Navar LG.** Nitric oxide dependency of arterial pressure-induced changes in renal interstitial hydrostatic pressure in dogs. *Circ Res* 88: 347–351, 2001.
62. **Majid DSA, Williams A, Kadowitz PJ, Navar LG.** Renal responses to intra-arterial administration of nitric oxide donor in dogs. *Hypertension* 22: 535–541, 1993.
63. **Majid DSA, Williams A, Navar LG.** Inhibition of nitric oxide synthesis attenuates pressure-induced natriuretic responses in anesthetized dogs. *Am J Phyisol Renal Fluid Electrolyte Physiol* 264: F79–F87, 1993.
64. **Marvar PJ, Hammer LW, Boegehold MA.** Hydrogen peroxide-dependent arteriolar dilation in contracting muscle of rats fed normal and high salt diets. *Microcirculation* 14: 779–791, 2007.
65. **Moss NG, Kopple TE, Arendshorst WJ.** Renal vasoconstriction by vasopressin V1a receptors is modulated by nitric oxide, prostanoids, and superoxide but not the ADP ribosyl cyclase CD38. *Am J Physiol Renal Physiol* 306: F1143–F1154, 2014.
66. **Nowicki PT, Flavahan S, Hassanain H, Mitra S, Holland S, Goldschmidt-Clermont PJ, Flavahan NA.** Redox signaling of the arteriolar myogenic response. *Circ Res* 89: 114–116, 2001.
67. **Ogawa N, Ono H.** Different effects of various vasodilators on autoregulation of renal blood flow in anesthetized dogs. *Jpn J Pharmacol* 41: 299–306, 1986.
68. **Ogawa N, Ono H.** Autoregulation of renal blood flow during the infusion of acetylcholine or carbachol in anaesthetized dogs. *J Pharm Pharmacol* 39: 493–495, 1987.
69. **Ozawa Y, Hayashi K, Wakino S, Kanda T, Homma K, Takamatsu I, Tatematsu S, Yoshioka K, Saruta T.** Free radical activity depends on underlying vasoconstrictors in renal microcirculation. *Clin Exp Hypertens* 26: 219–229, 2004.
70. **Park SW, Noh HJ, Sung DJ, Kim JG, Kim JM, Ryu SY, Kang K, Kim B, Bae YM, Cho H.** Hydrogen peroxide induces vasorelaxation by enhancing 4-aminopyridine-sensitive Kv currents through S-glutathionylation. *Pflügers Arch* 467: 285–297, 2015.
71. **Polichnowski AJ, Griffin KA, Long J, Williamson GA, Bidani AK.** Blood pressure-renal blood flow relationships in conscious angiotensin II- and phenylephrine-infused rats. *Am J Physiol Renal Physiol* 305: F1074–F1084, 2013.
72. **Pretus HA, Williams A, Navar LG.** Renal autoregulation is maintained during cytochrome P-450 inhibition in the dog (Abstract). *J Am Soc Nephrol* 4: 586, 1994.
73. **Raij L, Baylis C.** Glomerular actions of nitric oxide. *Kidney Int* 48: 20–32, 1995.

74. **Rajapakse NW, Mattson DL.** Role of cellular L-arginine uptake and nitric oxide production on renal blood flow and arterial pressure regulation. *Curr Opin Nephrol Hypertens* 22: 45–50, 2013.
75. **Ren Y, Carretero OA, Garvin JL.** Mechanism by which superoxide potentiates tubuloglomerular feedback. *Hypertension* 39: 624–628, 2002.
76. **Ren Y, D'Ambrosio MA, Liu R, Pagano PJ, Garvin JL, Carretero OA.** Enhanced myogenic response in the afferent arteriole of spontaneously hypertensive rats. *Am J Physiol Heart Circ Physiol* 298: H1769–H1775, 2010.
77. **Romero JC, Strick DM.** Nitric oxide and renal function. *Curr Opin Nephrol Hypertens* 2: 114–121, 1993.
78. **Sandner P, Kornfeld M, Ruan X, Arendshorst WJ, Kurtz A.** Nitric oxide/cAMP interactions in the control of rat renal vascular resistance. *Circ Res* 84: 186–192, 1999.
79. **Shi Y, Lau C, Cupples WA.** Interactive modulation of renal myogenic autoregulation by nitric oxide and endothelin acting through ET-B receptors. *Am J Physiol Regul Integr Comp Physiol* 292: R354–R361, 2007.
80. **Shi Y, Wang X, Chon KH, Cupples WA.** Tubuloglomerular feedback-dependent modulation of renal myogenic autoregulation by nitric oxide. *Am J Physiol Regul Integr Comp Physiol* 290: R982–R991, 2006.
81. **Siu KL, Sung B, Cupples WA, Moore LC, Chon KH.** Detection of low-frequency oscillations in renal blood flow. *Am J Physiol Renal Physiol* 297: F155–F162, 2009.
82. **Tolins JP, Palmer RMJ, Moncadea S, Raij L.** Role of endothelium-derived relaxing factor in regulation of renal hemodynamic responses. *Am J Physiol Heart Circ Physiol* 258: H655–H662, 1990.
83. **Trottier G, Triggle CR, O'Neill SK, Loutzenhiser RD.** Cyclic GMP-dependent and cyclic GMP-independent actions of nitric oxide on the renal afferent arteriole. *Br J Pharmacol* 125: 563–569, 1998.
84. **Vecchione C, Carnevale D, Di PA, Gentile MT, Damato A, Cocozza G, Antenucci G, Mascio G, Bettarini U, Landolfi A, Iorio L, Maffei A, Lembo G.** Pressure-induced vascular oxidative stress is mediated through activation of integrin-linked kinase 1/betaPIX/Rac-1 pathway. *Hypertension* 54: 1028–1034, 2009.
85. **Vogel PA, Yang X, Moss NG, Arendshorst WJ.** Superoxide enhances Ca^{2+} entry through L-type channels in the renal afferent arteriole. *Hypertension* 66: 374–381, 2015.
86. **Walker M III, Harrison-Bernard LM, Cook AK, Navar LG.** Dynamic interaction between myogenic and TGF mechanisms in afferent arteriolar blood flow autoregulation. *Am J Physiol Renal Physiol* 279: F858–F865, 2000.
87. **Wang X, Ajikobi DO, Salevsky FC, Cupples WA.** Impaired myogenic autoregulation in kidneys of Brown Norway rats. *Am J Physiol Renal Physiol* 278: F962–F969, 2000.
88. **Wang X, Cupples WA.** Interaction between nitric oxide and renal myogenic autoregulation in normotensive and hypertensive rats. *Can J Physiol Pharmacol* 79: 238–245, 2001.
89. **Wang X, Cupples WA.** Brown Norway rats show impaired nNOS-mediated information transfer in renal autoregulation. *Can J Physiol Pharmacol* 87: 29–36, 2009.
90. **Wang X, Loutzenhiser RD, Cupples WA.** Frequency modulation of renal myogenic autoregulation by perfusion pressure. *Am J Physiol Regul Integr Comp Physiol* 293: R1199–R1204, 2007.
91. **Wang X, Salevsky FC, Cupples WA.** Nitric oxide, atrial natriuretic factor, and dynamic renal autoregulation. *Can J Physiol Pharmacol* 77: 777–786, 1999.
92. **Welch PD.** The use of fast Fourier transform for the estimation of power spectra: a method based on time averaging over short, modified periodograms. *IEEE Trans Audio Electroacoustics* 15: 70–73, 1967.
93. **Welch WJ, Tojo A, Wilcox CS.** Roles of NO and oxygen radicals in tubuloglomerular feedback in SHR. *Am J Physiol Renal Physiol* 278: F769–F776, 2000.
94. **Wilcox CS.** Redox regulation of the afferent arteriole and tubuloglomerular feedback. *Acta Physiol Scand* 179: 217–223, 2003.
95. **Wronski T, Seeliger E, PErsson PB, Forner C, Fichtner C, Scheller J, Flemming B.** The step response: a method to characterize mechanisms of renal blood flow autoregulation. *Am J Physiol Renal Physiol* 285: F758–F764, 2003.
96. **Young DK, Marsh DJ.** Pulse wave propagation in renal tubules: implications for GFR autoregulation. *Am J Physiol Renal Fluid Electrolyte Physiol* 240: F446–F458, 1981.